Human Breast Cancer Transforming Growth Factor Beta (TGFβs) Pharmacophores Modeling and Virtual Screening Studies

Sudheer Kumar Reddy Poli [1], J.A.R.P Sarma[2],
Ramesh Raju[3], D.Sriniasa Rao[1], P.Sudhakar[1],
M.V.Raavendra Rao*[4]

Department of Biotechnology[1], Department of Chemistry[3], Acharya Nagarjuna University, GVK BIO[2], Hyderabad, Apollo Hospitals[4], Hyderabad, India.

ABSTRACT

In normal cells, TGF-β, acting through its signaling pathway, stops the cell cycle at the G1 stage to stop proliferation, induce differentiation, or promote apoptosis. When a cell is transformed into a cancer cell, parts of the TGF-β signaling pathway are mutated, and TGF-β no longer controls the cell. These cancer cells proliferate. The surrounding stromal cells (fibroblasts) also proliferate. Both cells increase their production of TGF-β. The pharmacophore generated can be used for the discovery of diversified structures that can be potential TGFRB1 inhibitors, and to evaluate how well any novel compound maps onto the pharmacophore developed during the study, using inhibitors against TGFRB1 possessing distinct features which may be responsible for the activity of the inhibitors. The models were not only predictive within the same series of compounds but different classes of diverse compounds were also effectively mapped onto most of the features important for activity. It can be generated as a Common feature pharmacophore and 3D QSAR pharmacophore. This TGF-β acts on the surrounding stromal cells, immune cells, and endothelial and smooth muscle cells. It causes immunosuppression and angiogenesis, which makes cancer more invasive. TGF-β also converts effector T-cells, which normally attack cancer with an inflammatory (immune) reaction, into regulatory (suppressor) T-cells, which turn off the inflammatory reaction.

INTRODUCTION

TGFβs can be detected in human breast cancer specimens. Moreover, tumor tissue appears to express higher levels of TGFβ than the corresponding normal tissue (1-4), and the association of TGFβs with cancer appears to be strongest in the most advanced stages of tumor progression (5). For example, TGFβ1, -2, and -3-specific mRNAs could be detected in the majority of primary breast cancers (6) and appeared to be more abundant than in normal breast tissue. In addition, several studies have reported immunostainable TGFβ1, -2, and -3 to be associated with the majority of primary human breast carcinomas (7). Furthermore, a significantly greater fraction of invasive carcinomas expressed immunodetectable TGFβ than in situ carcinomas (8), and the strongest staining was observed in invasive carcinomas with associated lymph node metastases, suggesting that there may be a semi-quantitative relationship between TGFβ production and tumor progression (9). Besides these reports of increased TGFβ expression in breast carcinomas (10), plasma levels of TGFβ have also been reported to be elevated in patients with breast cancer (11-12), to correlate with disease stage, and to decrease the following resection of the primary tumor (13-14). A common feature pharmacophore doesn't give us the estimated activities (15-17). Hence 3D QSAR pharmacophore models or quantitative pharmacophore models were generated in this study. These models can predict the activity values and are more dependable than the common feature pharmacophore.

Transforming growth factor (TGF-) is a multifunctional cell regulatory peptide that has varying effects on extracellular matrix synthesis, differentiation, proliferation, and tissue repair. At least three TGF-isoforms (TGF-1, -2, and -3) have been discovered in mammalian tissues, and it is known that these isoforms interact biologically with the two distinct TGF-R1 and TGF-R2 receptors (18). TGF- typically inhibits cell proliferation, but ironically, it may also have a significant role in fostering the onset of several malignant illnesses. Researchers have found evidence of TGF-overexpression in cancer cell lines grown in culture and the location of these cells in tumor tissues, and they have hypothesized that TGF has a strong stimulatory influence on the development of malignant epithelial neoplasms (19). Regarding mesenchymal neoplasms, TGF expression in various tumors that produce osteocartilaginous matrices, such as osteosarcomas and chondrosarcomas, has been studied. TGF- controls the synthesis of bone and cartilage by promoting the growth of osteoblasts and osteoclasts as well as the production of extracellular matrix in both healthy and malignant tissues (20). A pluripotent cytokine called transforming growth factor (TGF-beta) is involved in the

Citation: M.V.Raavendra Rao et al. Ijppr.Human, 2022; Vol. 25 (4): 661-681.

662

development, differentiation, adhesion, migration, and modulation of the immune response of cells (21).

MATERIALS AND METHODS

HYPOGEN (Training set)

Molecules collected from different databases were categorized into two sets a training set and a test set. Training set molecules were selected based on structure and activity diversity. The 24 molecules with activity values ranging from 0.002 µM - 31 µM (5-order magnitudes) were selected. The remaining molecules were treated as a test set, which consists of 48 molecules. Training set molecules contain an equal number of highest active, moderately active, and least active molecules. Each category of molecules has either structure diversity or activity diversity to represent the whole chemical space. After careful observation of the molecules, a few features were finalized for 3D QSAR pharmacophore hypothesis generation. The features selected for hypothesis model generation were given below.

Pharmacophore model validation using known TGFBR1 inhibitors

The validity of any pharmacophore model needs to be ascertained by screening some known inhibitors (test set) that are retrieved from the Kinase Inhibitor Databases to check how many active molecules are picked in the screening process, how their predicted activities are correlated with the experimental activities and the efficiency in reducing the false positives or negatives. Hypo-1 was used to screen 48 known high, medium, and low active TGFBR1 inhibitors of the test set. Database mining was performed in Catalyst software using the BEST flexible searching technique. Some parameters[42] such as hit list (Ht), number of active percent of yields (%Y), percent ratio of actives in the hit list (%A), enrichment factor of 1.83 (E), False negatives, False positives and Goodness of hit score of 0.78 (GH) are calculated (Table 1) while carrying out the pharmacophore model and virtual screening of test set molecules.
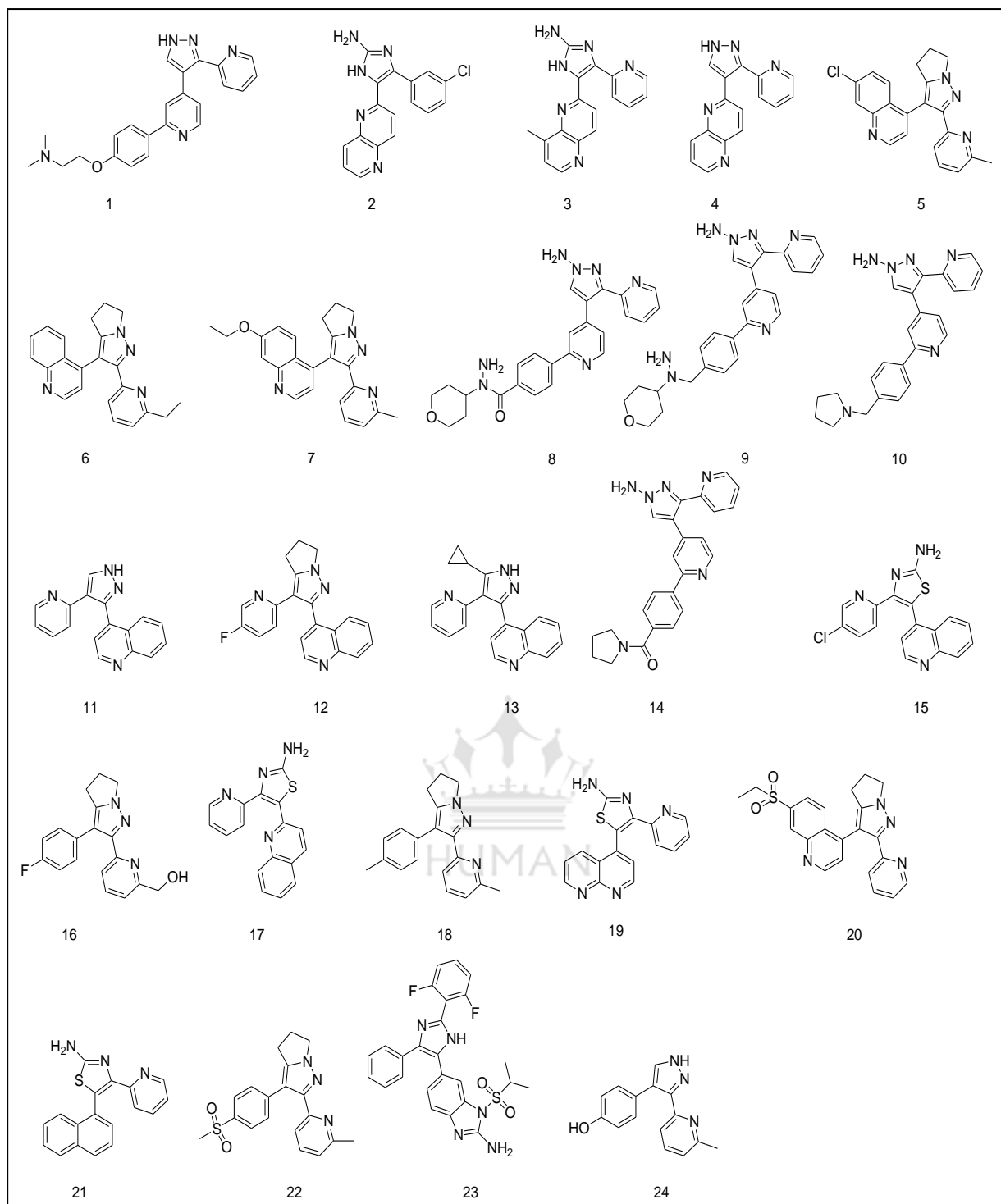
Citation: M.V.Raavendra Rao et al. Ijppr.Human, 2022; Vol. 25 (4): 661-681.

663

Figure no 1: Training set molecules used in pharmacophore generation

Citation: M.V.Raavendra Rao et al. Ijppr.Human, 2022; Vol. 25 (4): 661-681.

664

Table no 1: Statistical parameters from screening test set molecules.

S. No	Parameter	Molecules
1	Total molecules in the database (D)	48
2	Total Number of activities in the database (A)	23
3	Total Hits (H_t)	24
4	Active Hits (H_a)	21
5	% Yield of actives [(Ha/Ht)*100]	87.50
6	% Ratio of actives [(Ha/A)*100]	91.30
7	Enrichment factor (E) [(Ha*D)/(Ht*A)]	1.83
8	False Negatives [A - Ha]	2
9	False Positives [Ht - Ha]	3
10	The goodness of Hit Score	0.78

While the False positives and negatives, 3 and 2 respectively, are minimal, an enrichment factor of 1.83 is a good indication of the high efficiency of the screening. In 24 molecules predicted to be active, 21 molecules were correctly picked, thus missing only 2 false negatives with 3 false positives overall. GH score assessment of hit lists was used to optimize the working pharmacophore model as databases with known biological activities. It is to be noted that the technique can also be used to focus a list of active molecules as a post-HTS processing or to prioritize a virtual library as a pre-HTS screening.

Database Screening

The representative pharmacophore hypothesis (Hypo 1) was used as a search query to retrieve compounds with novel structural scaffolds and desired chemical features from a multi-conformer Catalyst-formatted database. This database is developed using ~1 million compounds present in the GVK BIO in-house database. The Fast Flexible Search Databases/Spread Sheets method in Catalyst was used to search the database.

Virtual Library screening studies

The Hypo-1 model was used to screen the Asinex database consisting of ~4M molecules, which yielded 4927 hits comprising 324 high, 1726 medium, and 2877 low active molecules. The highly active molecules were those <1 μM, moderately active (1-10 μM), and inactive

Citation: M.V.Raavendra Rao et al. Ijppr.Human, 2022; Vol. 25 (4): 661-681.

665

(>10 μM). Only 324 hits are found to be having activities below 0.1 μM cut-offs. One can consider all the 324 hits that are predicted to be highly active could become a good source for further evaluation, while some others in medium activities cannot be completely neglected. Some of the hits with good predicted activities were further subjected to docking studies to reduce the number of false positives and false negatives. Based on the earlier observations and the model developed in this study, it is observed that this virtual screening effort produced relatively more hits on which further experimental studies could be carried out. A few molecules with high predicted activity and Predicted activity are given in Figure **2.**
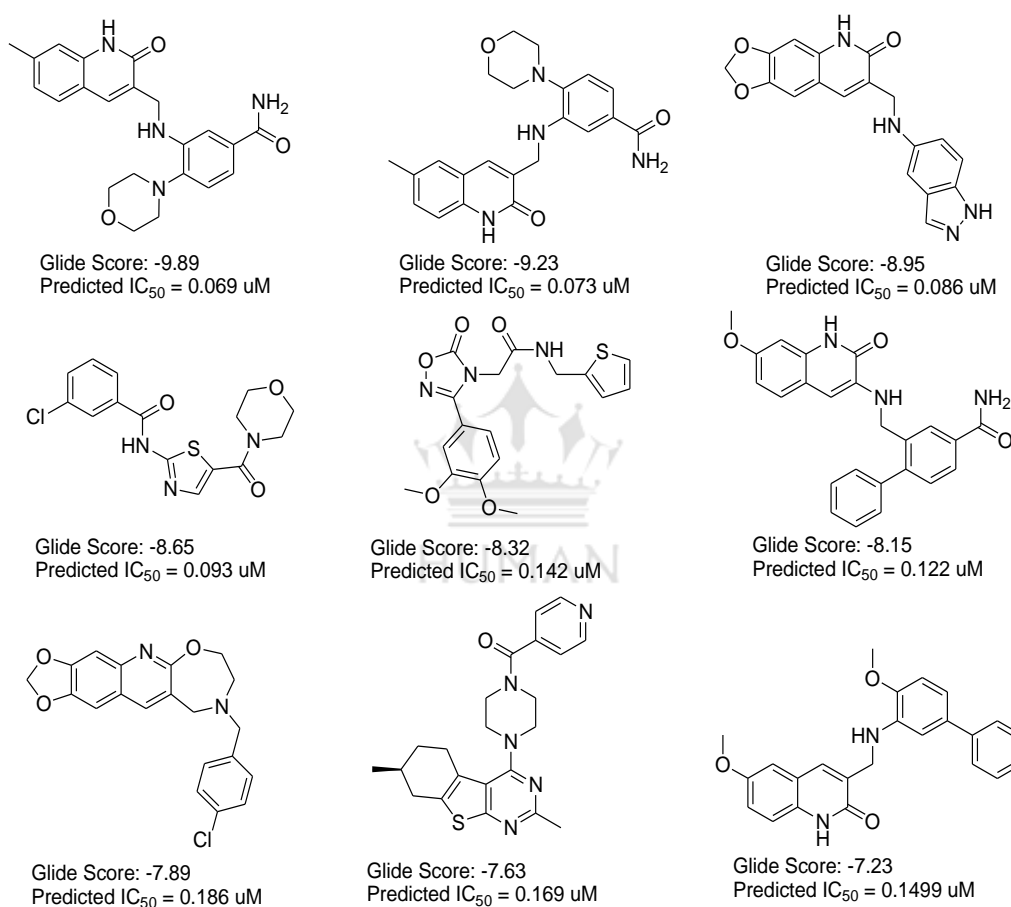

Figure no 2: Molecules retrieved from the Asinex database with predicted TGFRB1 inhibitory activity along with its GLIDE score values.

Validation of pharmacophore model using Test set molecules:

A library of molecules with known activities was taken for the validation of the selected best pharmacophore model. This set of molecules contains 48 molecules, their activity values range from 0.002 μM-31 μM. Structures of test set molecules were given below. We score the hypothesis based on fit values and regression plot generation. This hypothesis scoring

Citation: M.V.Raavendra Rao et al. Ijppr.Human, 2022; Vol. 25 (4): 661-681.

666

gives the estimated activity values as well as fit values. Better the fit value greater the activity. The later correlation was observed between the experimental activities and pharmacophore model predicted activities, which shows a good correlation i.e., **0.832**.
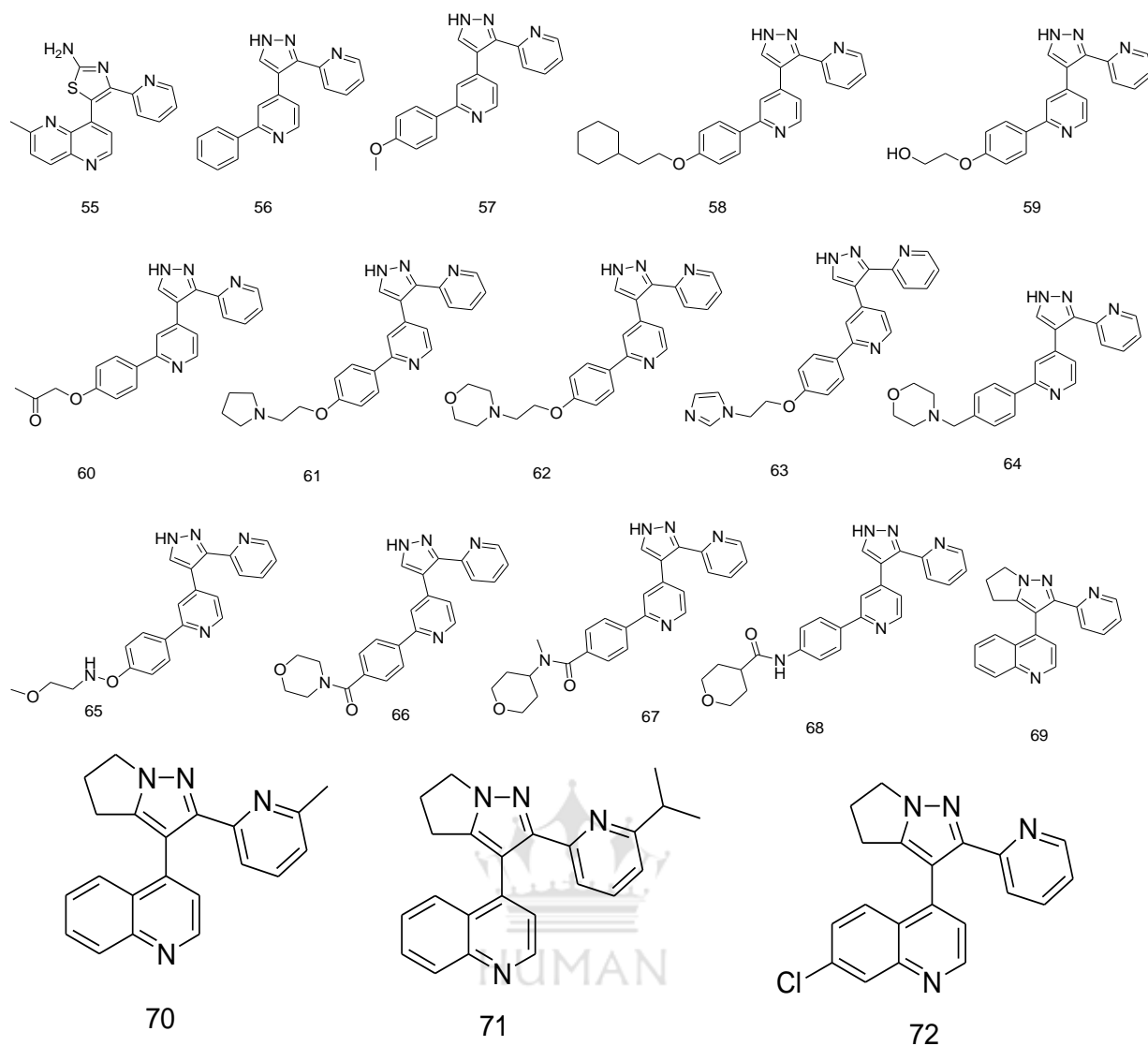
Citation: M.V.Raavendra Rao et al. Ijppr.Human, 2022; Vol. 25 (4): 661-681.

667
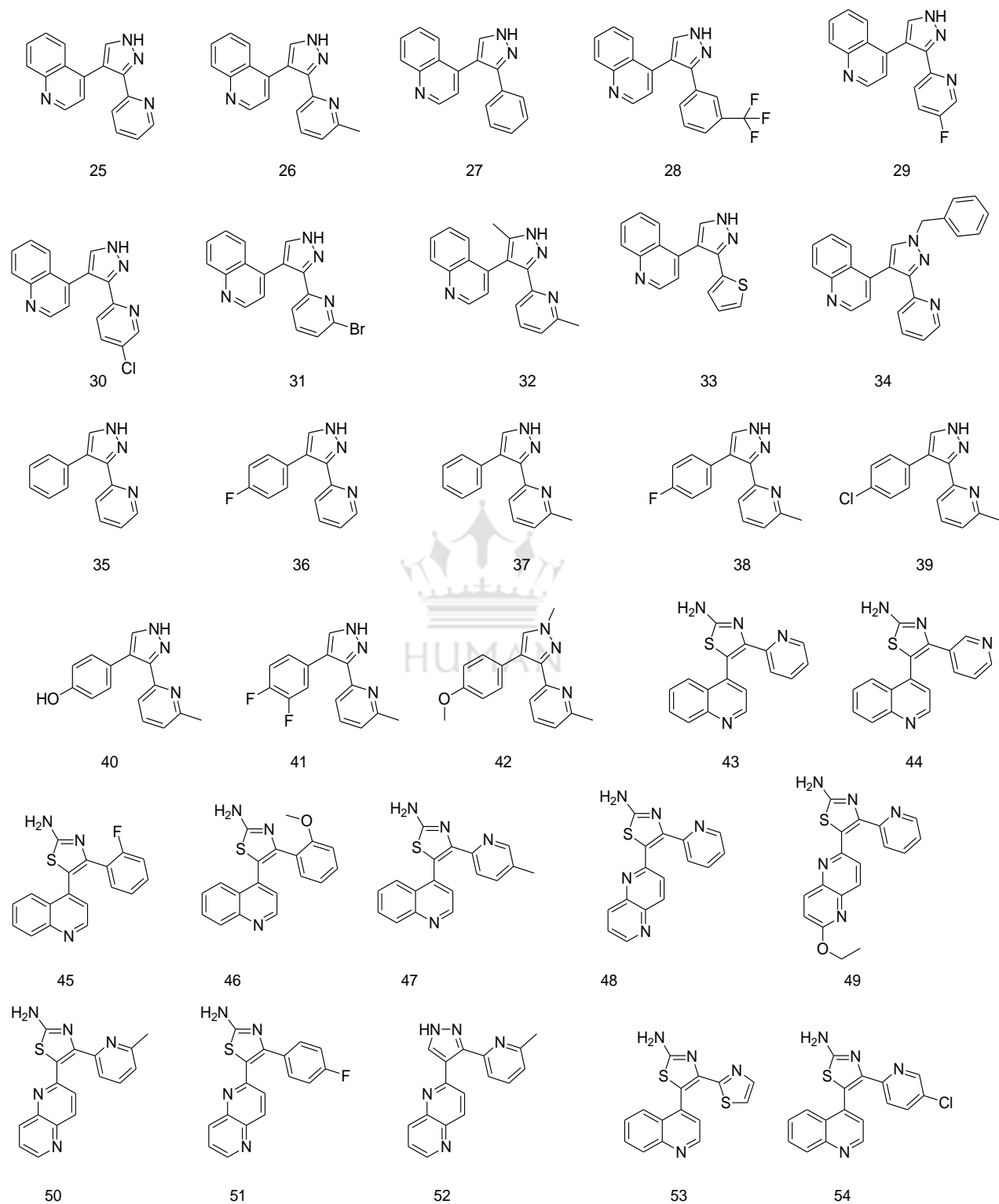
Figure no 3: Showing the test set molecules used in the pharmacophores model (Hypo1) validation

RESULTS AND DISCUSSION

A set of ten statistically significant pharmacophores (hypotheses) models was generated using 24 training set compounds and features mentioned above. Details of different pharmacophores hypotheses generated were listed in the below table.

Citation: M.V.Raavendra Rao et al. Ijppr.Human, 2022; Vol. 25 (4): 661-681.

668

Table no 2: Statistical significance of pharmacophore models generated using HypoGen

Hypo NO	Total cost	Cost-difference	RMS	Correlation®
1	**109.382**	**107.571**	**1.274**	**0.932**
2	116.514	100.439	1.454	0.911
3	120.806	96.147	1.570	0.896
4	124.597	92.356	1.767	0.863
5	127.048	89.905	1.793	0.859
6	127.614	89.339	1.823	0.854
7	141.771	75.182	2.135	0.793
8	146.97	69.983	2.254	0.765
9	148.713	68.24	2.266	0.762
10	150.645	66.308	2.304	0.753

Fixed cost: 85.953; Configuration cost: 15.155; Null cost: 216.953

All the above ten hypotheses were having a good correlation between actual or experimental activity and the activity predicted by the pharmacophores hypotheses in the training set. All the models have less RMS values indicating that they have good correlation. All the pharmacophores hypotheses have a cost difference greater than 60, which indicates that the models generated have more than a 90% correlation. All the hypotheses have cost components very close to ideal pharmacophores hypotheses. Where the cost difference was measured as the difference between the Null cost and the total cost of the pharmacophores hypotheses;

Cost difference = Null cost-total cost

The best pharmacophores are taken as hypothesis 1 based on internal validation. The best pharmacophores hypothesis has the highest cost difference (109.382), lowest error cost, lowest RMS difference (1.274), and the best correlation coefficient (0.932). This Pharmacophores hypothesis has one hydrogen bond acceptor, two hydrophobic features, and one hydrogen bond donor feature. The best pharmacophores have the highest cost difference of 107.571. The following figure shows the features present in the best pharmacophores hypothesis (Hypothesis-1). Pharmacophores features present in the best pharmacophores hypothesis were color-coded with green, cyan, and orange colors representing the hydrogen-bond acceptor feature, hydrophobic feature, and ring aromatic features respectively.

Citation: M.V.Raavendra Rao et al. Ijppr.Human, 2022; Vol. 25 (4): 661-681.

669

Table no 3: Features present in the Best pharmacophores model selected from top scoring ten pharmacophore models using HypoGen

S. NO	Feature name	Feature indication	No. of features	Colour indication
1	Hydrogen-bond acceptor	HBA	1	Green
2	Hydrophobic feature	H	2	Cyan
3	Ring Aromatic	RA	1	Orange
Total number of features4				

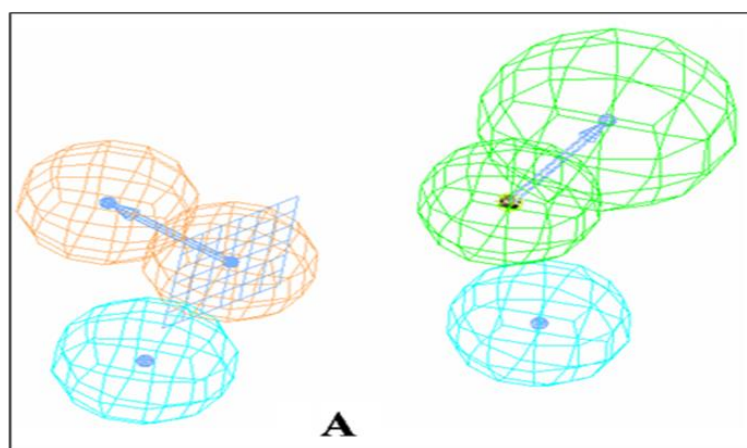**Hypo1:1HBA+2HY+1RA**

Figure no 4: (A) **The best hypothesis model Hypo1 produced by the 3D QSAR pharmacophores generation module in D.S 2.5 software**.
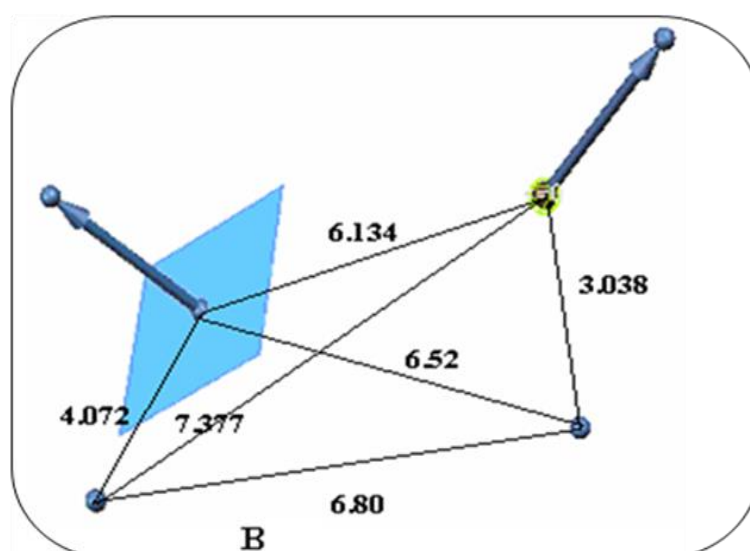

Figure no 5: Showing the 3D arrangement of pharmacophores features.

Citation: M.V.Raavendra Rao et al. Ijppr.Human, 2022; Vol. 25 (4): 661-681.

670

Distance between pharmacophores features is reported in angstroms. Ring aromatic and Acceptor features have projections. Hydrophobic features show only spheres. Ring aromatic feature showing plane also.

Table.no 4: 3D geometrical arrangement of features in Angstrom units

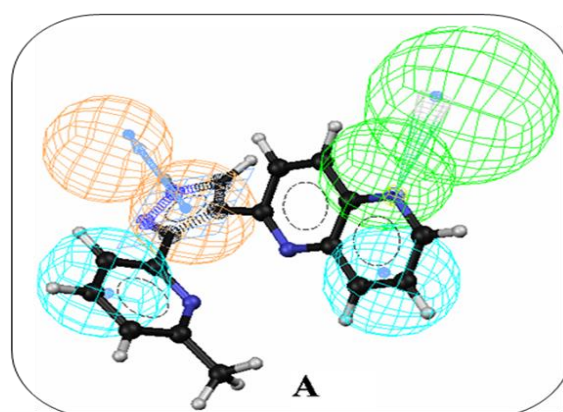| S. No	Features	Distance in A^0
1	Hydrophobic1 and Hydrophobic2 features	6.80
2	Hydrophobic1 and Ring aromatic features	4.072
3	Hydrophobic1 and Hydrogen bond Acceptor features	7.377
4	Hydrophobic2 and Ring aromatic features	6.52
5	Hydrophobic2 and Hydrogen bond Acceptor features	3.038
6	Hydrogen bond Acceptor and Ring aromatic features	6.134

Figure no 6. Mapping of the most active compound of the training set on the best Pharmacophores hypothesis model (Hypo 1)
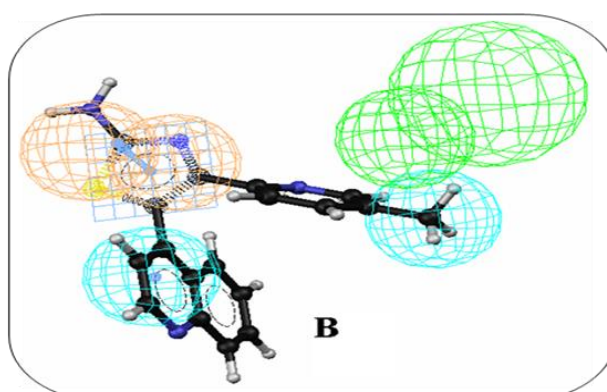

Figure no 7: Mapping of the least active compound of the training set on the best Pharmacophores hypothesis model (Hypo 1)

Citation: M.V.Raavendra Rao et al. Ijppr.Human, 2022; Vol. 25 (4): 661-681.

671

Best Model: Hypothesis-1 has the following statistical parameters to show its internal validity.

i. Cost difference: 107.571

ii. Training set correlation coefficient: 0.932.

Table no 4: Actual or Experimental activities and Quantitative pharmacophores model estimated activity values of training set molecules used for pharmacophores model generation

Compound No	Actual Activity (IC$_{50}$, uM)	Estimated Activity (IC$_{50}$, uM)
1	0.014	0.067
2	0.023	0.054
3	0.03	0.043
4	0.03	0.082
5	0.048	0.096
6	0.071	0.06
7	0.088	0.075
8	0.093	0.14
9	0.1	0.11
10	0.12	0.13
11	0.15	0.45
12	0.15	0.076
13	0.2	0.045
14	0.54	0.11
15	1	1.8
16	2.6	7.9
17	3.5	4.7
18	4	6.4
19	7.9	5
20	9.3	4.9
21	11	3.2
22	16	17
23	20	14
24	31	5.3

Citation: M.V.Raavendra Rao et al. Ijppr.Human, 2022; Vol. 25 (4): 661-681.
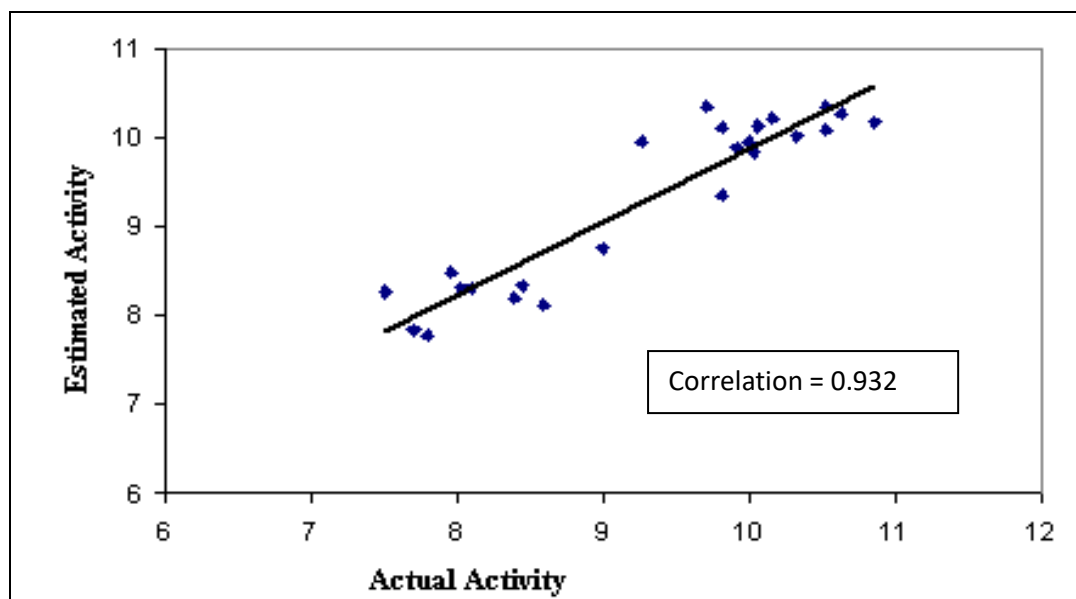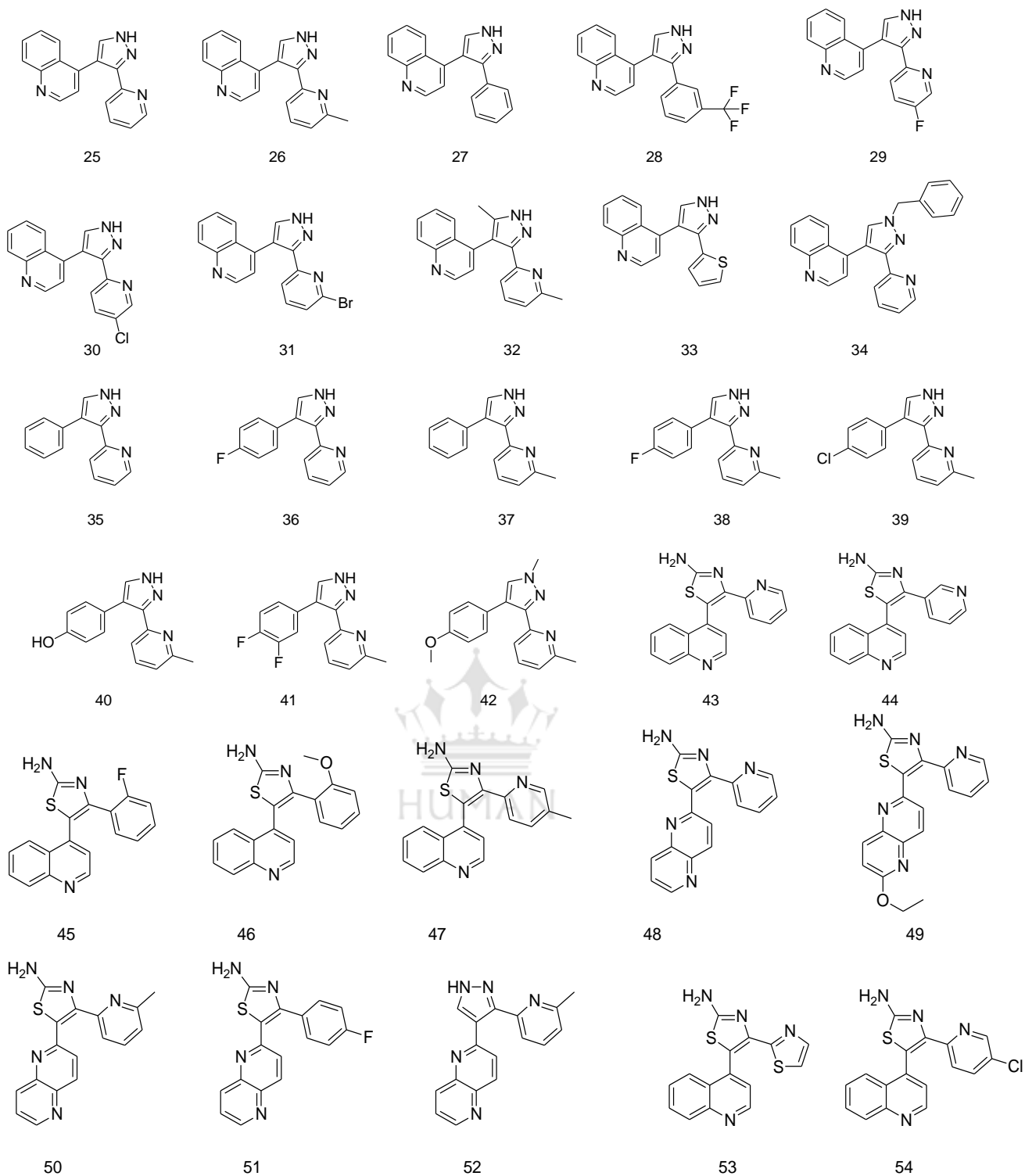
672

Figure no 8: Correlation graph between experimental and Hypo 1-estimated activities of training set molecules

Validation of pharmacophores model using Test set molecules:

A library of molecules with known activities was taken for the validation of selected best pharmacophores model. This set of molecules contains 48 molecules, their activity values range from 0.002 μM-31 μM. Structures of test set molecules were given below. We score the hypothesis based on fit values and regression plot generation. This hypothesis scoring gives the estimated activity values as well as fit values. Better the fit value greater the activity. Later correlation was observed between the experimental activities and pharmacophores model predicted activities, which shows good correlation i.e., **0.832**.
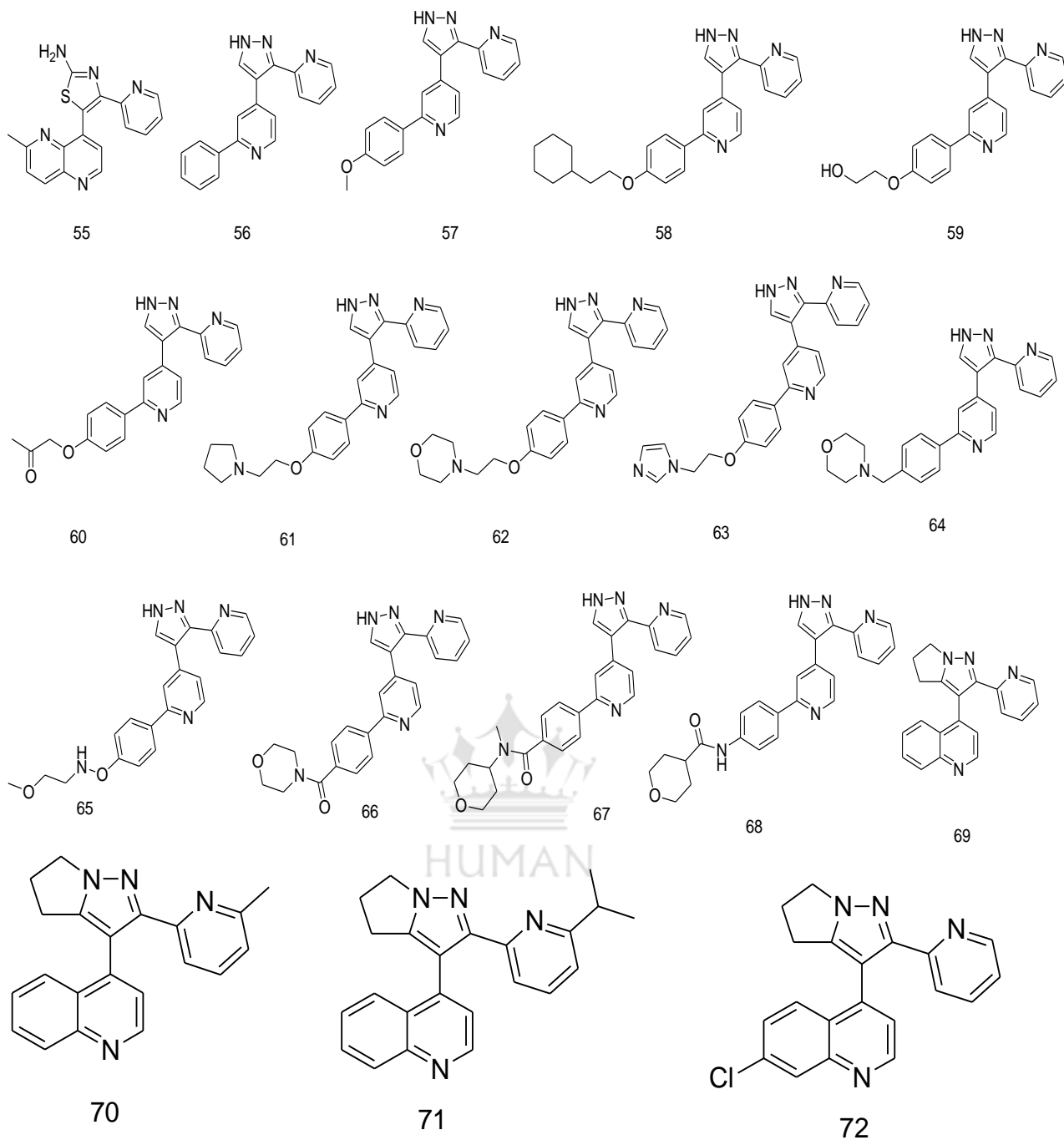
Citation: M.V.Raavendra Rao et al. Ijppr.Human, 2022; Vol. 25 (4): 661-681.

673

25

26

27

28

29

30

31

32

33

34

35

36

37

38

39

40

41

42

43

44

45

46

47

48

49

50

51

52

53

54

Citation: M.V.Raavendra Rao et al. Ijppr.Human, 2022; Vol. 25 (4): 661-681.

674

Figure no 9: Showing the test set molecules used in pharmacophores model (Hypo1) validation

Citation: M.V.Raavendra Rao et al. Ijppr.Human, 2022; Vol. 25 (4): 661-681.
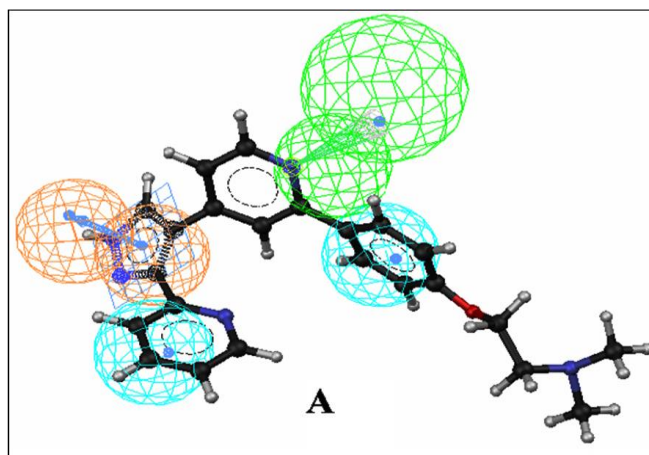
675

Figure no 10: Pharmacophores mapping of the most active compound of test set with hypothesis model Hypo 1
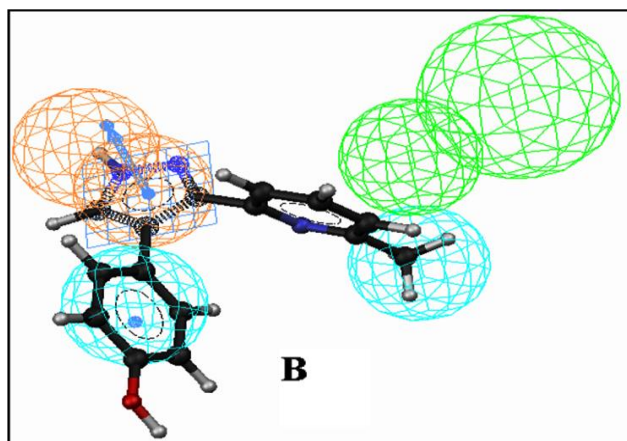

Figure no 11: **Pharmacophores mapping of the least active compound of test set with best hypothesis model Hypo 1**
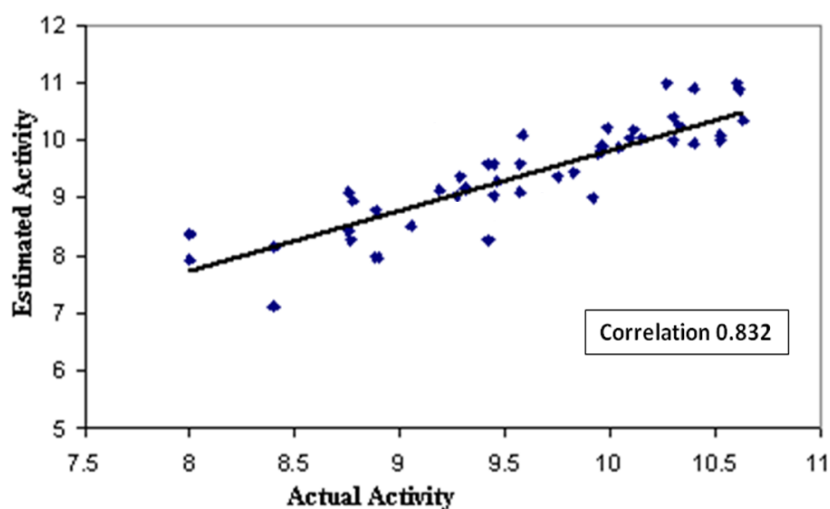

Figure no 12: Showing correlation (R = 0.832) graph between experimental and Hypo 1-estimated activities (uM) of the test set.

Citation: M.V.Raavendra Rao et al. Ijppr.Human, 2022; Vol. 25 (4): 661-681.

676

Docking Studies

The crystal structure of TGFBR1 (PDB ID: 1PY5) was used for the docking studies. The protein 3D structure was downloaded from the protein databank (PDB)[124]. The hydrogen atoms were added to the proteins and further minimization was performed. The reliability of this docking method to predict the bioactive conformation was validated using the X-ray structure of TGFRB1 in complex with a co-crystal molecule 4-(3-pyridin-2-yl-1h-pyrazol-4-yl) quinoline (PY1). Co-crystal PY1 re-docked into the active site of TGFRB1 and the best conformation with the lowest docking score was selected as the most probable conformation. The superimposition of the docking pose of PY1 with the co-crystal of 1PY5 is shown in figure 13 the root-mean-square deviation (RMSD) between these two poses is 0.497. A set of 72 human TGFBR1 inhibitors was docked into the active site of TGFBR1 using the Glide docking program. The TGFBR1 grid boxes were defined by the center of the bound inhibitors of the proteins. The enclosing box and binding box dimensions were fixed to 14Å, 14 Å, and 14 Å, respectively. The top 20 poses were collected for each compound. Docking poses were energy minimized using the OPLS-2001 force field. The best pose was selected based on the Glide score and the favorable interactions formed between the compound and amino acid residues of the TGFBR1 active site. The entire set of 72 inhibitors was docked into the active site of TGFBR1 and the correlation was calculated between the glide score and the IC50 by linear regression analysis method. An acceptable correlation coefficient (r2) of 0.78 was obtained between experimental IC50 and docking score (**Fig. 13**). This correlation strongly indicates that the binding conformations and binding models of the TGFRB1 inhibitors of TGFRB1 are reliable.
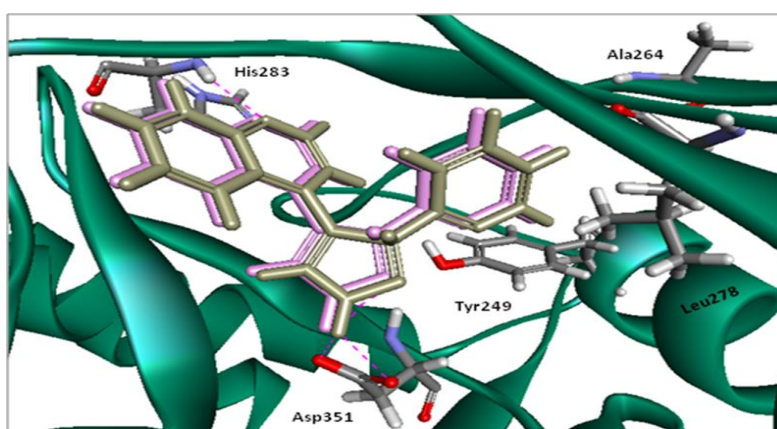

Figure: 13. **Superimposition of crystal ligand (pink) of 1PY5 and predicted binding pose (grey) of crystal ligand generated**.

Citation: M.V.Raavendra Rao et al. Ijppr.Human, 2022; Vol. 25 (4): 661-681.
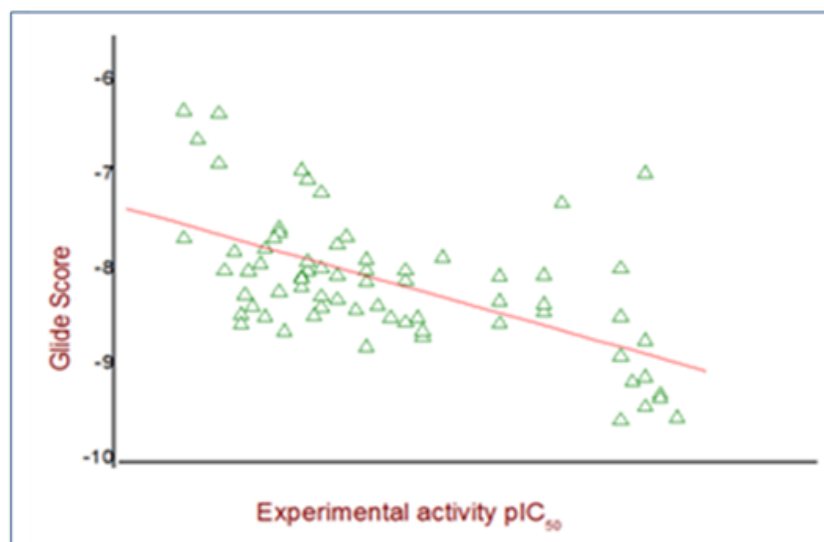
677

Figure 14 Graphical representation of the correlation between dock score and experimental activity of TGFBR1 inhibitors

The high-fit value compounds obtained from the virtual screening of the Asinex database are docked into the TGFBR1 protein active site. The compounds are ranked based on score. The best predicted bound compounds are given in Figure 15. The compound-1 is binding to the protein active site and making hydrogen bond interaction with the main chain of His283 (2.3 Å). The compound-3 is binding to the protein active site and making hydrogen bond interaction with the main chain of His283 (2.37 Å). The compounds-5 is binding to the protein active site and making hydrogen bond interaction with the main chain of His283 (2.80 Å) and two more hydrogen bond interactions with Ser 280, one with main chain nitrogen (2.71 Å), another hydrogen bond interaction with side chain OH (2.02 Å) and one more hydrogen bond interaction with nitrogen present in the side chain of Lys232 (2.8 Å). The compounds-7 is binding to the protein active site and making hydrogen bond interaction with the main chain of His283 (2.53 Å) and two more hydrogen bond interactions with Ser 280, one with main chain nitrogen (2.92), another hydrogen bond interaction with side chain OH(1.62 Å). The predicted binding poses of a few high active compounds are given in **Figure 15.** The compounds are making hydrogen bonding interactions with TGFBR1 similar to that of crystal ligands and have a high binding affinity towards TGFBR1.
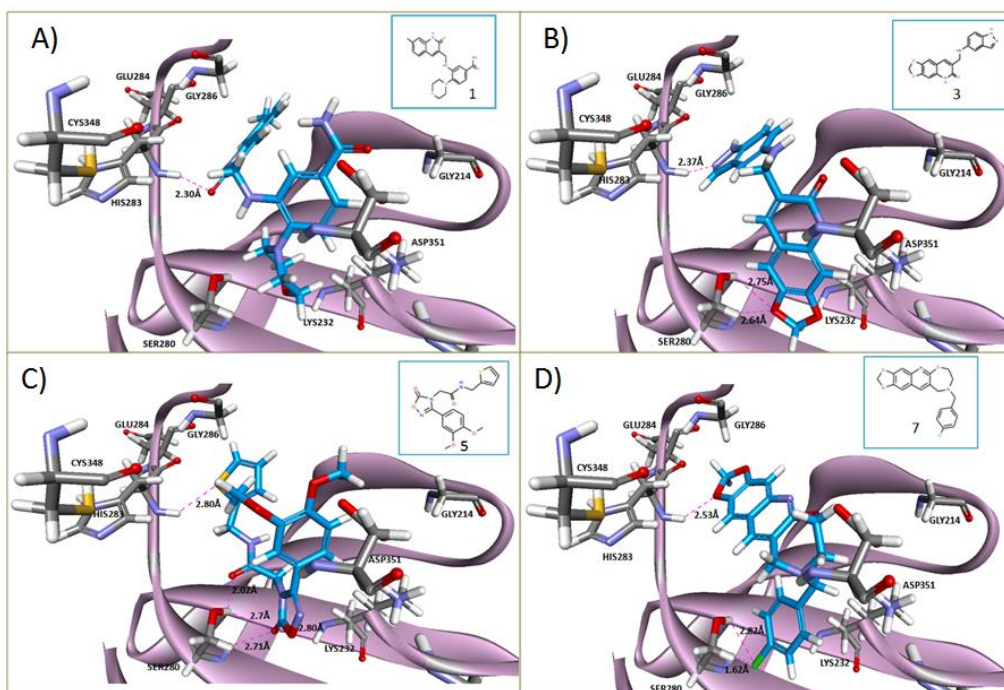
Citation: M.V.Raavendra Rao et al. Ijppr.Human, 2022; Vol. 25 (4): 661-681.

678

Figure no 15. Predicted binding mode of Compound-1(A),3(B),5(C), and 7 (D) obtained from docking studies.

CONCLUSION

The pharmacophores and docking models were generated and validated utilizing a set of known TGFBR1 inhibitors. Compounds bearing agreeable chemical and structural features are potential leads for designing strategies targeting TGFBR1. The models were not only predictive for the same series of compounds but also for different classes of diverse compounds where they were effectively mapped onto most of the features important for activity. In conclusion, it has been shown that modification of typical pharmacophores and a combination of Pharmacophores and docking-based virtual screening methods can improve the activity and result in identifying competitive and reversible inhibitors of TGFBR1. From the docking and virtual screening methods and from Pharmacological studies 9 hits were identified. The pharmacophore model is further used to screen putative molecules from the Asinexdatabase. An astute blend of pharmacophore analysis, docking procedures, and database search have resulted in predicting putative novel inhibitors of the TGFBR1. We have finally identified 9 hits from *In Silico* studies.

Citation: M.V.Raavendra Rao et al. Ijppr.Human, 2022; Vol. 25 (4): 661-681.

679

REFERENCES

1. Sminia P, Barten AD, van Waarde MA, Vujaskovic Z, van Tienhoven G. Plasma transforming growth factor beta levels in breast cancer patients. Oncol Rep 1998;5(2):485–488.

2. Sheen-Chen SM, Chen HS, Sheen CW, Eng HL, Chen WJ. Serum levels of transforming growthfactor beta1 in patients with breast cancer. Arch Surg 2001;136(8):937–940.

3. Kong FM, Anscher MS, Murase T, Abbott BD, Iglehart JD, Jirtle RL. Elevated plasma transforminggrowth factor-beta 1 levels in breast cancer patients decrease after surgical removal of the tumor.Ann Surg 1995; 222(2):155–162.

4. Grau AM, Wen W, Ramroopsingh DS, Gao YT, Zi J, Cai Q, et al. Circulating transforming growthfactor-beta-1 and breast cancer prognosis: results from the Shanghai breast cancer study. BreastCancer Res Treat 2007;106:205–213.

5. Baselga J, Rothenberg ML, Tabernero J, Seoane J, Daly T, Cleverly A, et al. TGF-beta signalling-related markers in cancer patients with bone metastasis. Biomarkers 2008;13(2):217–236.

6. Chakravarthy D, Green AR, Green VL, Kerin MJ, Speirs V. Expression and secretion of TGF-betaisoforms and expression of TGF- beta-receptors I, II and III in normal and neoplastic human breast.Int J Oncol 1999;15(1):187–194.

7. Gobbi H, Dupont WD, Simpson JF, Plummer WD Jr, Schuyler PA, Olson SJ, et al. Transforminggrowth factor-beta and breast cancer risk in women with mammary epithelial hyperplasia. J NatlCancer Inst 1999;91(24):2096–2101.

8. Gobbi H, Arteaga CL, Jensen RA, Simpson JF, Dupont WD, Olson SJ, et al. Loss of expression oftransforming growth factor beta type II receptor correlates with high tumour grade in human breastin-situ and invasive carcinomas. Histopathology 2000;36(2):168–177.

9. Buck MB, Fritz P, Dippon J, Zugmaier G, Knabbe C. Prognostic significance of transforming growthfactor beta receptor II in estrogen receptor-negative breast cancer patients. Clin Cancer Res 2004;10(2):491–498.

10. Shipitsin M, Campbell LL, Argani P, Weremowicz S, Bloushtain-Qimron N, Yao J, et al. Moleculardefinition of breast tumor heterogeneity. Cancer Cell 2007;11(3):259–273.

11. Wang Y, Klijn JG, Zhang Y, Sieuwerts AM, Look MP, Yang F, et al. Gene-expression profiles topredict distant metastasis of lymph-node-negative primary breast cancer. Lancet 2005;365(9460):671–679.

12. Padua D, Zhang XH, Wang Q, Nadal C, Gerald WL, Gomis RR, et al. TGFbeta primes breast tumorsfor lung metastasis seeding through angiopoietin-like 4. Cell 2008;133(1):66–77.

13. Takenoshita S, Mogi A, Tani M, Osawa H, Sunaga H, Kakegawa H, et al. Absence of mutations inthe analysis of coding sequences of the entire transforming growth factor-beta type II receptor genein sporadic human breast cancers. Oncol Rep 1998;5(2):367–371.

14. Chen T, Carter D, Garrigue-Antar L, Reiss M. Transforming growth factor beta type I receptorkinase mutant associated with metastatic breast cancer. Cancer Res 1998;58(21):4805–4810.

15. Lucke CD, Philpott A, Metcalfe JC, Thompson AM, Hughes-Davies L, Kemp PR, et al. Inhibitingmutations in the transforming growth factor beta type 2 receptor in recurrent human breast cancer. Cancer Res 2001;61(2):482–485.

16. Baxter SW, Choong DY, Eccles DM, Campbell IG. Transforming growth factor beta receptor 1polyalanine polymorphism and exon 5 mutation analysis in breast and ovarian cancer. CancerEpidemiol Biomarkers Prev 2002;11(2):211–214.

17. Kang JS, Saunier EF, Akhurst RJ, Derynck R. The type I TGF- β receptor is covalently modifiedand regulated by sumoylation. Nat Cell Biol 2008;10(6):654–664.

18. Yamamoto K, Yoshida K, Miyagoe Y, et al. Quan-titative evaluation of expression of iron-metabo-lism genes in ceruloplasmin-deficient mice. Bio-chimBiophys Acta. 2002;1588:195-202.

19. Murthy L, Menden EE, Eller PM, Petering HG. Atomic absorption determination of zinc, copper, cadmium, and lead in tissues solubilized by aqueous tetramethylammonium hydroxide. Anal Bio-chem. 1973;53:365-372.

20. He W, Dorn DC, Erdjument-Bromage H, Tempst P, Moore MA, Massague J. Hematopoiesis con-trolled by distinct TIF1gamma and Smad4 branches of the TGFbeta pathway. Cell. 2006; 125:929-941.

Citation: M.V.Raavendra Rao et al. Ijppr.Human, 2022; Vol. 25 (4): 661-681.

680

21. Carlino JA, Higley HR, Creson JR, Avis PD, Ogawa Y, Ellingsworth LR. Transforming growth factor beta 1 systemically modulates granuloid, erythroid, lymphoid, and thrombocytic cells in mice. Exp Hematol. 1992;20:943-950.

Citation: M.V.Raavendra Rao et al. Ijppr.Human, 2022; Vol. 25 (4): 661-681.

681